1991

Solid State Proton Spin Relaxation in Ethylbenzenes: Methyl Reorientation Barriers and Molecular Structure

Peter A. Beckmann
Bryn Mawr College, pbeckman@brynmawr.edu

Laura Happersett

Antonia V. Herzog

William M. Tong

Solid state proton spin relaxation in ethylbenzenes: Methyl reorientation barriers and molecular structure

Peter A. Beckmann, Laura Happersett, Antonia V. Herzog,[a] and William M. Tong[b]

Department of Physics, Bryn Mawr College, Bryn Mawr, Pennsylvania 19010

We have investigated the dynamics of the ethyl groups and their constituent methyl groups in polycrystalline ethylbenzene (EB), 1,2-diethylbenzene (1,2-DEB), 1,3-DEB, and 1,4-DEB using the solid state proton spin relaxation (SSPSR) technique. The temperature and Larmor frequency dependence of the Zeeman spin-lattice relaxation rate is reported and interpreted in terms of the molecular dynamics. We determine that only the methyl groups are reorienting on the nuclear magnetic resonance time scale. The observed barrier of about 12 kJ/mol for methyl group reorientation in the solid samples of EB, 1,2-DEB, and 1,3-DEB is consistent with that of the isolated molecule, implying that in the solid state, intermolecular electrostatic interactions play a minor role in determining the barrier. The lower barrier of 9.3 ± 0.2 kJ/mol for the more symmetric 1,4-DEB suggests that the crystal structure is such that the minimum in the anisotropic part of the intramolecular potential is raised by the intermolecular interactions leading to a 3 kJ/mol *decrease* in the total barrier. We are able to conclude that the methyl group is well away from the plane of the benzene ring (most likely orthogonal to it) in all four molecules, and that in 1,2-DEB, the two ethyl groups are in the *anti*configuration. Our SSPSR results are compared with the results obtained by microwave spectroscopy and supersonic molecular jet laser spectroscopy, both of which determine molecular geometry better than SSPSR, but neither of which can determine ground electronic state barriers for these molecules.

I. INTRODUCTION

We have investigated the dependence on temperature and Larmor angular frequency of the proton Zeeman spin–lattice relaxation rate in polycrystalline ethylbenzene (EB), 1,2-diethylbenzene (1,2-DEB), 1,3-DEB, and 1,4-DEB. A schematic picture of EB, $C_6H_5CH_2CH_3$, is shown in Fig. 1. Solid state proton spin relaxation (SSPSR) is a useful technique for (1) studying low barriers for molecular reorientation; (2) modeling intramolecular motion and determining the statistics of the reorientation process; (3) studying the dynamic effects of molecular packing in the solid state; and (4) studying solid–solid phase transitions. In this paper, we are concerned with the first three of these matters.

In solids, methyl groups reorient in a wide variety of intramolecular and intermolecular environments. Hindering barriers for methyl groups in aryllike molecular solids range from about 1 kJ/mol[1,2] to quite high barriers in strongly sterically crowded environments.[3] The barriers for methyl reorientation in the molecules studied here are in the range 9–15 kJ/mol, depending only slightly (about ± 1 kJ/mol) on the specific models used to interpret the data. One strength of the SSPSR technique lies in the fact that barriers down to about 3 kJ/mol can be measured above liquid nitrogen temperatures (77 K) and considerably lower barriers down to about 0.5 kJ/mol can be measured at lower temperatures.[4] In SSPSR studies, it is nuclear magnetic reso-

nance activation energies that are measured, but in most models these can usually be identified with reorientation barriers to within reasonable accuracy.[5,6] Barriers below about 20 kJ/mol are difficult to study by dilute liquid high resolution nuclear magnetic resonance (NMR) spectroscopy.[7-9] From the measurement of a sufficient number of appropriate J couplings in high resolution NMR spectra, barriers in the range of 0.8–13 kJ/mol can be determined in very limited cases.[10] These cases do *not* include threefold rotational barriers for methyl groups. Inelastic neutron scattering techniques can determine barriers over a wide range at low temperatures in the solid state where tunneling rather than thermally activated rotation is the dominant reorientation process.[11-13] Finally, barriers below about 15 kJ/mol are difficult to study by computational techniques.[14]

II. EXPERIMENT

All four samples were obtained from Aldrich Chemical. They are all liquids at room temperature. The melting points and the quoted purities are 178 K, 99% for EB; 242 K, 95% for 1,2-DEB; 189 K, 99% for 1,3-DEB; and 230 K, 96% for 1,4-DEB. The samples were used without further purification. It is clear from the relaxation rate data that paramagnetic impurities, if present, were inconsequential. In these kinds of organic compounds, where the dialkyl systems have impurities at the level of 4% or 5%, the impurities are usually other isomers and this has a negligible effect on the interpretation of the data.

Proton Zeeman spin–lattice relaxation rates R were measured from 77 K to the melting point at 8.5, 22.5, and 53 MHz using three fixed-frequency Spin-Lock Model CPS-2

---

[a] Present Address: Department of Physics, University of California at San Diego, La Jolla, Ca. 92093.

[b] Present Address: Department of Chemistry and Biochemistry, University of California at Los Angeles, Los Angeles, Ca. 90024.
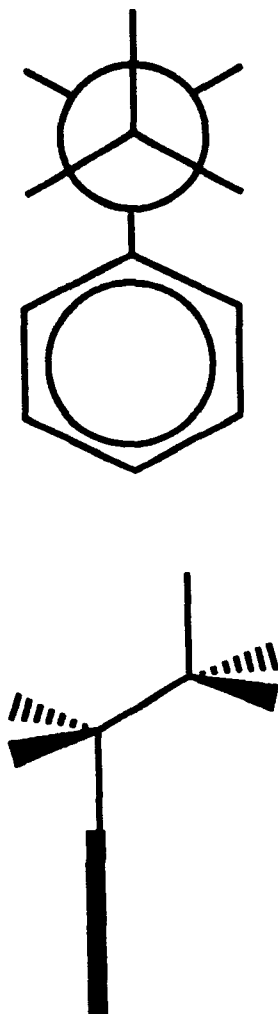
FIG. 1. A schematic picture of ethylbenzene (EB). The methyl group is shown in the "orthogonal" position. The top picture shows a Newman projection for the ethyl group.
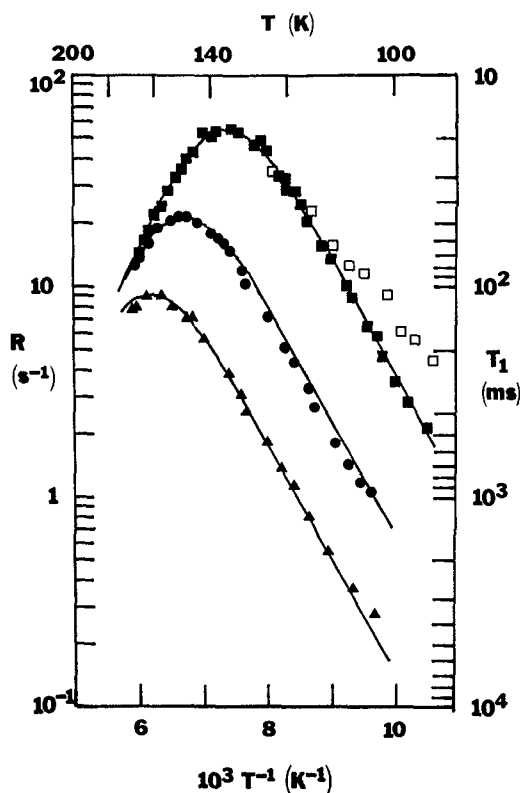
FIG. 2. The temperature T dependence of the proton Zeeman relaxation rates R at Larmor frequencies of 8.5 (■,□), 22.5 (●), and 53 MHz (▲) in ethylbenzene (EB). Closed symbols indicate the polycrystalline state and open symbols indicate the glassy state. The full lines indicate fit 1.

spectrometers. Standard techniques were employed. The data are shown in Figs. 2–5. To within experimental uncertainty, the relaxation was exponential for EB (Fig. 2) and 1, 2-DEB (Fig. 5). In this case, the uncertainty in the observed rates R is about 5%, which is less than the scatter in adjacent data points on the ln R vs T^{-1} plots. The latter, therefore, should be taken as a measure of the uncertainty in R. For 1,3-DEB (Fig. 4) and 1,4-DEB (Fig. 3), the relaxation was nonexponential. In these cases, the R reported in Figs. 3 and 4 characterize the initial slope of the relaxation curve which was well defined in all cases, but more so for 1,3-DEB than for 1,4-DEB. As such, the uncertainties in R for 1,3-DEB (Fig. 4) are about 10% and the uncertainties in R for 1,4-DEB (Fig. 3) are about 20%. In both cases, a realistic measure of the uncertainties are given by the scatter in the ln R vs T^{-1} data.

Temperature was controlled by a flow of reheated cold nitrogen gas and temperature was monitored by a calibrated copper–constantan thermocouple. Temperature could be maintained to about ± 0.3 K and the uncertainty in the measurement of the absolute temperature is about ± 1 K.

In preparing the samples, dry nitrogen gas was bubbled through them to displace dissolved oxygen which can give rise to anomalous relaxation. The samples were usually fro-

zen slowly (i.e., over a period of minutes) to form a crystalline state.[15] This did not matter for 1,2-DEB and 1,4-DEB for which the same R vs T^{-1} data were obtained if the sample was frozen quickly (i.e., emersed in liquid nitrogen). For EB and 1,3-DEB, however, a different R vs T^{-1} data set was

FIG. 3. The temperature T dependence of the proton Zeeman relaxation rates R at Larmor frequencies of 8.5 (■), 22.5 (●), and 53 MHz (▲) in polycrystalline 1,4-diethylbenzene (1,4-DEB). The full lines indicate fits 2 and 4 and the dashed lines indicate fit 3.

FIG. 4. The temperature T dependence of the proton Zeeman relaxation rates R at Larmor frequencies of 8.5 (■, □), 22.5 (●,○), and 53 MHz (▲) in 1,3-diethylbenzene (1,3-DEB). Closed symbols indicate the polycrystalline state and open symbols indicate the glassy state. The full lines indicate fit 5. Fit 6 is essentially the same.
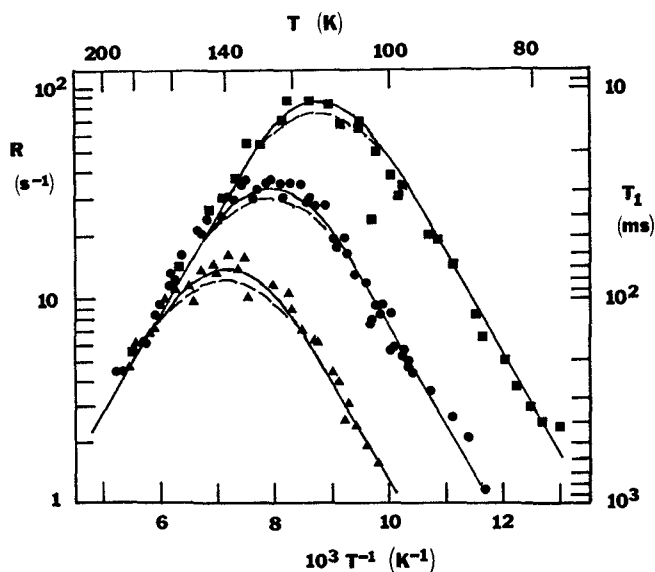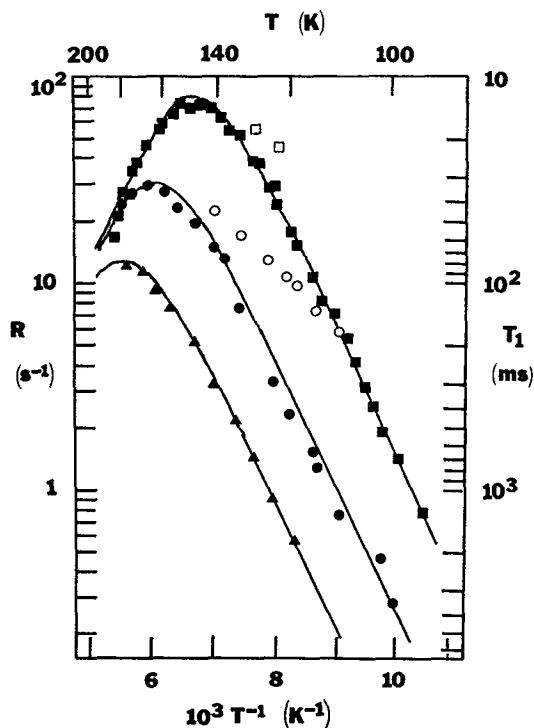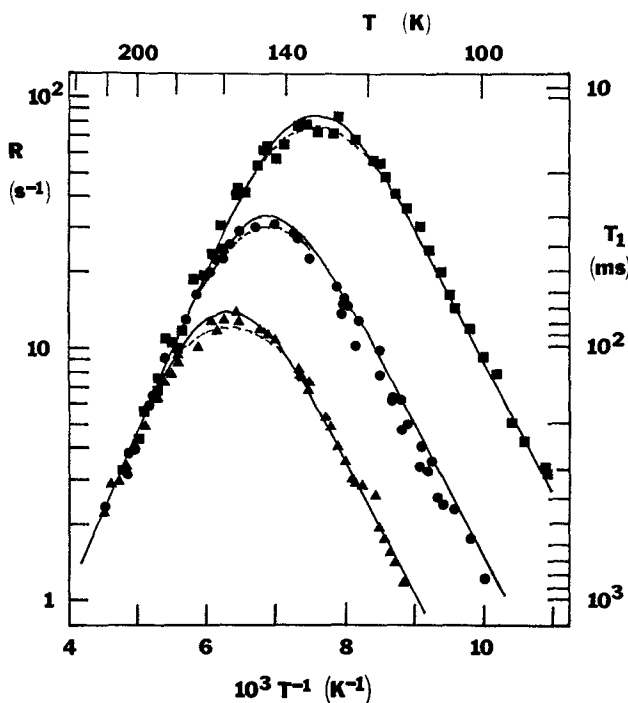

FIG. 5. The temperature T dependence of the proton Zeeman relaxation rates R at Larmor frequencies of 8.5 (■), 22.5 (●), and 53 MHz (▲) in polycrystalline 1,2-diethylbenzene (1,2-DEB). The full lines indicate fits 7 and 10. Fit 8 is essentially the same. The dashed lines indicate fit 9.

obtained for the fairly quickly (several seconds) frozen samples which were presumably in a glassy state. These results are consistent with lower melting points for EB (178 K) and 1,3-DEB (189 K) compared with those for 1,2-DEB (242 K) and 1,4-DEB (230 K). If one takes the ratio of boiling point to melting point, they are 2.4 (1,3-DEB), 2.2 (EB), 2.0 (1,4-DEB), and 1.9 (1,2-DEB), so the formation of a glass state in our case is consistent with the empirical rule that glass states tend to form more easily if this ratio is above about 2.0.[16,17] We show a few R vs T^{-1} data points for these glassy states as open symbols in Figs. 2 and 4.

III. THEORY

We develop a model for the proton spin–lattice relaxation rate $R = T_1^{-1}$ due to methyl and ethyl group reorientation. Since the spin–spin interaction is very much stronger than the spin–lattice interaction (i.e., $R_2 \gg R$, where $R_2 = T_2^{-1}$ is the spin–spin relaxation rate), spin diffusion keeps the spin system in internal equilibrium and the *observed* rate R is then associated with the average[18,19]

$$R = \frac{2}{N} \sum_{\substack{i=1 \\ i<j}}^{N} \sum_{j=2}^{N} \mathscr{R}_{ij}. \tag{1}$$

$\mathscr{R}_{ij}$ is the relaxation rate for an ensemble of ij spin pairs. N is the total number of spins in the system (molecule) and therefore depends on the molecule under study. For EB, $N = 10$, and for the three isomers of DEB, $N = 14$.

We note that, in general, for three strongly coupled spin-1/2 particles like the protons in a methyl group, a perturbed nuclear Zeeman magnetization will not relax exponentially, but rather via a sum of exponentials even though $R_2 \gg R$. This is because the motions of the three proton–proton vectors are completely correlated and there are cross-correlation terms as well as autocorrelation terms in the correlation function that describes the motion.[20-22] We assume that all such cross correlation terms are zero. In some of the experiments reported here (1,3-DEB and 1,4-DEB), nonexponential relaxation is observed. In this case, the single relaxation rates to be used in Eq. (1) are appropriate to the initial relaxation (i.e., small times) where autocorrelations dominate and cross correlations can be neglected.[20]

R in Eq. (1) has $(1/2)N(N-1)$ terms (45 for EB and 91 for DEB). We assume that the only possible motion involves the ethyl group (or groups) and its constituent methyl group. It is unlikely that in the solid state, whole-molecule reorientation will occur on the nuclear magnetic resonance time scale. Even if it did, it would have a small effect on the magnitude of R, as discussed elsewhere for *t*-butylbenzene,[18] although it might change significantly the time-averaged intermolecular component of the electrostatic potential seen by the ethyl groups.

We assume that interactions between ethyl protons and nonethyl protons can be neglected as can the interactions between protons on different ethyl groups. This reduces the number of interactions to (10)n for a molecule with n ethyl groups. Given that the relaxation rate is proportional to the various spin–spin separations r according to r^{-6} (see be-

low), this is a reasonable assumption consistent with the experimental data. Note that this specifically excludes all intermolecular dipole–dipole interactions.

R in Eq. (1) is divided into three terms

$$R = R_m + R_p + R_{mp}, \qquad (2)$$

where R_m is the relaxation rate resulting from the modulation, by both ethyl and methyl group reorientation, of the intramethyl dipole–dipole interactions. R_p is the relaxation rate resulting from the modulation, by ethyl group reorientation only, of the interaction between the two ethyl, nonmethyl protons. R_{mp} is the relaxation rate resulting from the modulation of the interaction between the methyl protons and the two ethyl nonmethyl protons.

In general, the reorientation of the proton–proton vector r_{ij} between the proton pairs ij is characterized by a parameter set $\{x_k\}_{ij} \equiv \{x_1, x_2, x_3, \ldots\}_{ij}$ that depends on the electrostatic interactions. It is assumed that there is an ensemble of such pairs in the usual statistical mechanical manner. In the simplest models, the set $\{x_k\}_{ij}$ reduces to the parameter τ_{ij} for correlation time τ_{ij}. (The parameter τ_{ij} is model dependent and may, in turn, be parametrized by more than one parameter.) These times τ_{ij} can be identified with the mean time between hops in a random process. If the process involves different sets of random processes, then these correlation times are model dependent and must be defined. Later, we will use a model that requires one additional dynamical parameter in addition to a correlation time τ_{ij}.

R_m has been presented elsewhere.[18] It takes into account methyl reorientation characterized by correlation time τ_m and ethyl group reorientation characterized by correlation time τ_e.

$$R_m = \frac{2}{N} 3n \frac{3}{20} \left(\frac{\mu_0}{4\pi}\right)^2 \frac{\gamma^4 \hbar^2}{r_m^6} \left[\tfrac{2}{9} q(\omega, \tau_m) + \tfrac{2}{9} q(\omega, \tau_e) \right.$$
$$\left. + \tfrac{12}{36} q(\omega, \tau_{me}) \right], \qquad (3)$$

where n is the number of methyl or ethyl groups in the molecule and N is the number of hydrogen atoms in the molecule. The factor $\mu_0/(4\pi) \equiv 10^{-7}$ m kg s^{-2} A^{-2}, where μ_0 is the permeability of free space. The distance $r_m = 0.180$ nm is the intramethyl group proton–proton separation. The function q is given by[23]

$$q(\omega, \tau) = J(\omega, \tau) + 4J(2\omega, \tau) \qquad (4)$$

and the spectral density J is appropriately normalized.[24] J depends on the Larmor angular frequency $\omega = \gamma B$, where B is the applied magnetic field and $\gamma = 2.675 \times 10^8$ kg^{-1} s A is the magnetogyric ratio of the proton. Specific forms for J are reviewed elsewhere.[24]

The superposition correlation time τ_{me} in Eq. (3) is

$$\tau_{me}^{-1} = \tau_m^{-1} + \tau_e^{-1}. \qquad (5)$$

If there is no ethyl group reorientation, $\tau_e^{-1} = o$, $q(\omega, \tau_e) = 0$, $\tau_{me} = \tau_m$, and Eq. (3) reduces to

$$R_m = \frac{2}{N} 3n \frac{3}{20} \frac{3}{4} \left(\frac{\mu_0}{4\pi}\right)^2 \frac{\gamma^4 \hbar^2}{r_m^6} q(\omega, \tau_m), \qquad (6)$$

which is the relaxation rate for a reorienting methyl group in a molecule with a total of n methyl groups and N protons.

Cast in the form of Eq. (1), Eq. (6) is $R_m = (2/N)(3n\mathscr{R})$, there being $3n$ terms in the sum in Eq. (1). The rate $\mathscr{R}$, in this case, is the relaxation rate resulting from the reorientation of a single proton–proton vector in the methyl group. It follows then that R_p in Eq. (2), the relaxation rate resulting from the modulation of the dipole–dipole interaction between the two nonmethyl protons in the ethyl group, is given by Eq. (6) without the factor of 3 in $3n$ and with τ_m replaced by τ_e:

$$R_p = \frac{2}{N} n \frac{3}{20} \frac{3}{4} \left(\frac{\mu_0}{4\pi}\right)^2 \frac{\gamma^4 \hbar^2}{r_m^6} q(\omega, \tau_e), \qquad (7)$$

where n now refers specifically to the number of ethyl groups.

We use an approximation for the relaxation rate R_{mp} in Eq. (2). Whereas the magnitudes of the intramethyl and the intraethyl, nonmethyl proton–proton vectors are constant, the magnitudes of the six intraethyl, methyl–nonmethyl proton–proton vectors are rendered time dependent by methyl and/or ethyl group reorientation. We approximate the contribution of these terms by imagining the three protons in the methyl group to be condensed to the center of the methyl group triangle.[25] With this approximation, the "effective" proton–proton distance is $r_{me} = 0.250$ nm, assuming an idealized ethyl group geometry which we are doing throughout this analysis. All six terms in the sum over $\mathscr{R}_{ij}$ in Eq. (1) are identical and only ethyl reorientation modulates the interactions. R_{mp} follows from Eq. (6) and is given by

$$R_{mp} = \frac{2}{N} 6n \frac{3}{20} \frac{3}{4} \left(\frac{\mu_0}{4\pi}\right)^2 \frac{\gamma^4 \hbar^2}{r_{me}^6} q(\omega, \tau_e). \qquad (8)$$

If the motion is random and all reorienting units are in dynamically equivalent environments, then the distribution of times between hops characterizing the methyl and/or ethyl group hopping process will be given by a Poisson distribution characterized by the mean hop rate τ^{-1}. The spectral density J in this case is[23]

$$J_{\text{BPP}}(\omega, \tau) = \frac{2\tau}{1 + \omega^2 \tau^2}, \qquad (9)$$

after Bloembergen, Purcell, and Pound.[26] The correlation time τ is related to the temperature via an Arrhenius relationship

$$\tau = \tau_\infty e^{E/kT}, \qquad (10)$$

which introduces the activation energy (barrier) E and the preexponential factor τ_∞.

The spectral density in Eq. (9) will often not fit experimental data because there is a distribution of correlation times, each characterizing a Poisson process. This will lead to a non-BPP spectral density. This situation is quite likely to occur either because the crystal structure itself gives rise to several environments[27] or because imperfections and crystallite boundaries in the polycrystalline sample give rise to a distribution of environments. It is also possible that some or all of the sample is in a glassy state in which case there would also be a distribution of ethyl group environments, and therefore a distribution of barriers for reorientation. We think that it is unlikely that the data we will proceed to fit (presented as solid symbols in Figs. 2–5) are representative

of the glassy state because (a) the results were reproducible; (b) the samples were frozen slowly; (c) if two of the samples were frozen quickly, a different state with a different R vs T^{-1} signature was obtained (open symbols in Figs. 2 and 4, presumably the glassy state); and (d) the distribution of correlation times we will use is extremely narrow (see Fig. 6) as discussed later.

A general spectral density can be formed from a distribution of BPP spectral densities, each characterized by a correlation time ξ. The spectral density becomes

$$J(\omega, x_1, x_2, \ldots) = \int_0^\infty \Lambda(\xi, x_1, x_2, \ldots) \frac{2\xi}{1 + \omega^2 \xi^2} d\xi, \quad (11)$$

where the distribution function Λ is appropriately normalized.[24]

We use the spectral density due to Davidson and Cole[28] (DC) mainly because it is successful, easy to use, and only introduces one additional parameter ϵ, which characterizes the width of the distribution. It is obtained from Eq. (11) with a distribution $\Lambda(\xi, \tau, \epsilon)$ given by

$$\Lambda_{DC}(\xi, \tau, \epsilon) = \sin(\epsilon\pi) \frac{1}{\pi\xi} \left(\frac{\xi}{\tau - \xi} \right)^\epsilon, \quad \xi < \tau$$
$$= 0, \quad \xi > \tau. \quad (12)$$

Equations (11) and (12) give the spectral density

$$J_{DC}(\omega, \tau) = \frac{2}{\omega} \frac{\sin[\epsilon \arctan(\omega\tau)]}{(1 + \omega^2\tau^2)^{\epsilon/2}}, \quad (13)$$

which is discussed in detail elsewhere.[24] The parameter τ becomes a cut-off correlation time and is assumed to be modeled by Eq. (10) for cut-off activation energy E and cut-off infinite temperature correlation time τ_∞. Corresponding to this (or any) distribution of correlation times ξ, there will be a distribution $\Gamma(\mathscr{E}, E, x_2, x_3, \ldots)$ of activation energies $\mathscr{E}$. Although it is not necessary to pursue this in order to fit the data, we do so in order to compare the simplest models for Γ with a Dirac δ function which is what Γ would be for a BPP distribution leading to the spectral density in Eq. (9). The

relationship between $\Gamma(\mathscr{E}, E, x_2, x_3, \ldots)$ and the distribution of correlation times $\Lambda(\xi, \tau, x_2, x_3, \ldots)$ can be defined formally via

$$\Gamma(\mathscr{E}, E, x_2, x_3, \ldots) d\mathscr{E} = \Lambda(\xi, \tau, x_2, x_3, \ldots) d\xi, \quad (14)$$

but until the relationship between the correlation time ξ and the activation energy $\mathscr{E}$ is modeled, Λ cannot be determined. We assume that

$$\xi = \xi_\infty e^{\mathscr{E}/kT}, \quad (15)$$

in analogy with Eq. (10) for τ, which is the cut-off value of ξ. Unless the form of ξ_∞ in Eq. (15) is known, $d\mathscr{E}/d\xi$ cannot be determined, even if $\Lambda(\xi, \tau, x_2, x_3, \ldots)$ is known. As a result, $\Gamma(\mathscr{E}, E, \epsilon)$ for the DC spectral density cannot be determined. As a model, we assume that the dependence of ξ_∞ on $\mathscr{E}$ and T is weak compared with the dependence of ξ on $\mathscr{E}$ and T via the exponential in Eq. (15). If it is assumed further that ξ_∞ in Eq. (15) is constant and equal to the cutoff τ_∞, then Eqs. (12), (14), and (15) give

$$\Gamma_{DC}(\mathscr{E}, E, \epsilon) = \frac{\sin(\epsilon\pi)}{\pi(kT)} \left(\frac{1}{e^{(E - \mathscr{E})/kT} - 1} \right)^\epsilon, \quad \mathscr{E} < E$$
$$= 0, \quad \mathscr{E} > E; \quad (16)$$

where $0 < \epsilon \leqslant 1$.

When $\epsilon = 1$, the DC spectral density J_{DC} in Eq. (13) reduces to the BPP spectral density J_{BPP} in Eq. (9). An example of Γ for $\epsilon = 0.85$ is shown in Fig. 6. We emphasize that there is no fundamental theoretical justification for the DC spectral density, although one could argue that the cut-off E corresponds to the barrier for rotors in "perfect" crystal sites and the range of $\mathscr{E} < E$ corresponds to the barrier for rotors at crystallite boundaries, imperfections, etc. In any event, the distribution is very narrow, but the logarithmic singularity at $\mathscr{E} = E$ and an absolute cutoff at E is essential to fit the data. No symmetric distribution, regardless how narrow, will suffice.[24]

IV. DATA ANALYSIS

We test several models for the dynamics and conclude that only the methyl groups are reorienting on the nuclear magnetic resonance time scale. Assuming first that only methyl group reorientation is occurring, the observed relaxation rate is given by Eq. (6) which, for convenience, we rewrite

$$R = \frac{n}{N} \tilde{A}_m q(\omega, \tau_m), \quad (17)$$

with $\tilde{A}_m = 1.14 \times 10^{10}$ s^{-2}. [We denote theoretical values of A and τ_∞ with a tilde (i.e., $\tilde{A}$ and $\tilde{\tau}_\infty$) and fitted values without a tilde.] The choice of normalization makes $\tilde{A}_m$ independent of molecule. For 1,4-DEB (Fig. 3), the data (at all three frequencies) is well fitted by a single BPP spectral density. The fit (fit 2) is shown in Fig. 3 and the fitted values of $A_m/\tilde{A}_m$, E, and τ_∞ are given in Table I. The ratio $\tau_\infty/\tilde{\tau}_\infty$ is also given where the theoretical value $\tilde{\tau}_\infty$ is based on a very simple model which is reviewed elsewhere.[29] The physical origins of $\tilde{\tau}_\infty$ do not matter here, it is simply a convenient benchmark. Values of $\tau_\infty/\tilde{\tau}_\infty$ several orders of magnitude from unity would be suspect. The large uncertainty in all τ_∞
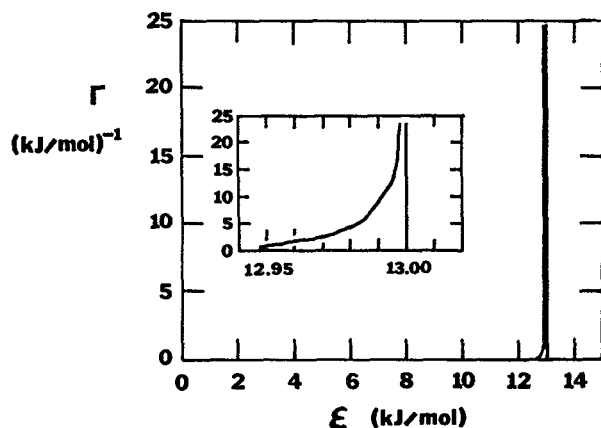

FIG. 6. The distribution of activation energies $\Gamma(\mathscr{E})$ vs $\mathscr{E}$ for the Davidson–Cole distribution with cutoff $E = 13$ kJ/mol, width parameter $\epsilon = 0.85$, and $T = 100$ K. The inset shows the range $12.95 < \mathscr{E} < 13.00$ kJ/mol on an expanded $\mathscr{E}$ scale and a compressed Γ scale.

TABLE I. Relaxation rate parameters for ethyl groups.

Fit	Molecule	E (kJ/mol)	$A/\tilde{A}$	ϵ	τ_∞ (s)	$\tau_\infty/\tilde{\tau}_\infty$
1	EB	13.2 ± 0.7	0.98	0.83 ± 0.04	$(1.3 \pm 0.7)\times 10^{-13}$	0.3–1.3
2	1,4-DEB	9.3 ± 0.2	1.0	1	$(6.5 \pm 0.4)\times 10^{-13}$	3.5–3.9
3	1,4-DEB	9.3 ± 0.2	0.54	1	$(8.3 \pm 0.5)\times 10^{-13}$	4.4–5.0
4	1,4-DEB	9.3 ± 0.2	3.4	1	$(6.5 \pm 0.4)\times 10^{-13}$	3.5–3.9
5	1,3-DEB	14.1 ± 0.5	1.0	0.85 ± 0.03	$(1.5 \pm 0.6)\times 10^{-13}$	0.6–1.5
6	1,3-DEB	15 ± 2	1.0	1	1×10^{-14}–5×10^{-13}	0.01–1
		12 ± 1	1.0	1	1×10^{-13}–1×10^{-12}	1–10
7	1,2-DEB	12.2 ± 0.2	1.1	0.84 ± 0.02	$(2.0 \pm 0.2)\times 10^{-13}$	1.1–1.5
8	1,2-DEB	13 ± 1	1.0	1	1×10^{-13}–2×10^{-13}	0.6–1.2
		11 ± 1	1.0	1	2×10^{-13}–5×10^{-13}	1.2–3.0
9	1,2-DEB	12.2 ± 0.2	0.55	0.84 ± 0.02	$(2.6 \pm 0.3)\times 10^{-13}$	1.4–1.9
10	1,2-DEB	12.2 ± 0.2	3.7	0.84 ± 0.02	$(2.0 \pm 0.2)\times 10^{-13}$	1.1–1.5

values are dominated by the uncertainty in E which appears in the exponential in the Arrhenius relationship.

A fit using a BPP spectral density [Eq. (9)] will not work for the other molecules and a DC spectral density [Eq. (13)] is used if Eq. (17) is used. The fits for EB (fit 1, solid lines in Fig. 2), 1,3-DEB (fit 5, solid lines in Fig. 4), and 1,2-DEB (fit 7, solid lines in Fig. 5) are very good. The A_m, E, τ_m, and ϵ are given in Table I. The distribution corresponding to the fitted values of ϵ is discussed below.

The values of $A_m/\tilde{A}_m$ for all of these fits (BPP for 1,4-DEB and DC for the other three molecules) are all unity or very close to unity and this implies that within the framework of this dynamical model, only intramethyl proton–proton interactions need be taken into account. Although the crystal structures are not known, this result is consistent with known distances between intramolecular methyl and nonmethyl protons and with reasonable estimates for distances between protons on different molecules. If several protons were very near to the methyl group, such as would be required if two methyl groups on nearby molecules were involved in a cooperative motion, the value of $A/\tilde{A}$ would be considerably larger.

The DC spectral density is mimicking a distribution of correlation times. Another model for the motion assumes the sum of two terms of the form of Eq. (17), but each with a BPP spectral density. The question is, can the distribution of activation energies in Fig. 6 be replaced by two Dirac δ functions? This might be the case if the crystal structure led to two inequivalent methyl group sites. A similar two-site model was proposed for tri-*t*-butylbenzene[30] and confirmed by an x-ray study.[31] In this case, there are six parameters A_m, E, and τ_∞ for each site. In practice, we force $A_{m1} = A_{m2} = \tilde{A}_{m1}(A_{m1}/\tilde{A}_{m1})$ with $\tilde{A}_{m1} = \tilde{A}_m/2 = 5.7 \times 10^9$ s^{-2} which is half the value for the one-site model. The single ratio $A_{m1}/\tilde{A}_{m1}$ is then the fitting parameter and there are five adjustable parameters. The parameters characterizing the fits for 1,3-DEB (fit 6) and 1,2-DEB (fit 8) are indicated in Table I and the fits are insignificantly different from fits 5 (1,3-DEB) and 7 (1,2-DEB) discussed previously. The larger uncertainties in the E values simply reflect the increased number of parameters. If one of the two E values is

set at a fixed value, the uncertainty in the other is much smaller than the 10% or so indicated. That is, the indicated uncertainties reflect the manner in which the two E values can be changed simultaneously in the fit. The data for EB cannot be successfully fitted in this manner and the procedure is not relevant for 1,4-DEB, where a single BPP fit is already successful.

On one hand, a value of ϵ in the vicinity of 0.85 is close enough to unity that the actual distribution of activation energies is extremely narrow (see Fig. 6). On the other hand, ϵ is the ratio of the magnitudes of the high to low temperature slopes $\Delta \ln R / \Delta T^{-1}$ (Ref. 29) and the fits are very sensitive to this parameter. The value $\epsilon = 0.85$ is significantly less than unity from this perspective and forcing $\epsilon = 1$ would lead to a very bad fit. This says that to the extent that ϵ in the DC spectral density is interpreted as a measure of the width of the distribution of activation energies, the SSPSR technique is very sensitive to this width.

Models which assume that the ethyl group and the methyl group are reorienting at the same rate will fit the data, but the resulting A values make no sense as we now show. The most general form for the observed relaxation rate is obtained by inserting Eqs. (3), (7), and (8) in Eq. (2). The result is rewritten in the form

$$R = \frac{1}{N}\sum_{i=1}^{n} [\tilde{A}_e q(\omega, \tau_{ei})$$
$$+ \tilde{A}'_m q(\omega, \tau_{mi}) + \tilde{A}_{em} q(\omega, \tau_{emi})] , \qquad (18)$$

where n is now the number of chemically distinct ethyl groups and N is the appropriate total number of protons. For example, if the crystal structure is such that there are four molecules of DEB per unit cell with eight distinct ethyl group sites, then $n = 8$ and $N = 56$, four times the number of protons per molecule. The ratio n/N will always be the same as the single molecule value. With these conventions, $\tilde{A}$ can be kept at the same molecule-independent values. The $\tilde{A}$ values in Eq. (18) are $\tilde{A}_e = 1.04\times 10^{10}$ s^{-2}, $\tilde{A}'_m = 3.39 \times 10^9$ s^{-2}, and $\tilde{A}_{em} = 8.04\times 10^9$ s^{-2}. [Note that if $\tau_{ei} = \infty$, the first term in Eq. (18) vanishes, $\tau_{mi} = \tau_{emi}$, and $\tilde{A}'_m + \tilde{A}_{em}$ in Eq. (18) equals $\tilde{A}_m$ in Eq. (17). This is why

the methyl terms in Eqs. (17) and (18) are different and a prime is used in the latter.] The several possible correlation times τ are given by Eq. (10) with the appropriate subscripts on the activation energy E and the infinite temperature correlation time τ_∞. If there were very different activation energies E_m and E_e involved with the two correlation times τ_m and τ_e, then two maxima in ln R vs T^{-1} would be observed.[32] As can be seen in Figs. 2–5, this is not the case. There are very few superimposed reorientation models which will fit the data and the range of possible E values can be estimated from fits 6 and 8 in Table I. One such model assumes that the reorientation of the methyl group and the ethyl group are characterized by the same correlation time due to some gearing mechanism. To be consistent with previous work with t-butyl groups, we call this an A-type ethyl group and the constituent methyl group an a-type methyl group. Both are characterized by τ_a and the correlation times $\tau_{ei} = \tau_{mi} = \tau_a$ and $\tau_{emi} = \tau_a/2$ for all i. Equation (18) reduces to

$$R = \frac{n}{N}\left[\tilde{A}_a q(\omega,\tau_a) + \tilde{A}_{aa} q(\omega,\tau_a/2)\right],\qquad(19)$$

with $\tilde{A}_a = \tilde{A}_e + \tilde{A}'_m = 1.38\times10^{10}$ s^{-2} and $\tilde{A}_{aa} = \tilde{A}_{em} = 8.04\times10^{10}$ s^{-2}. The two terms in Eq. (19) lead to an R vs T that is very similar to a single term,[32] differing by less than 10% in the vicinity of the maximum in R if the low- and high-temperature ln R vs T^{-1} regions from Eq. (19) and a single term fit are superimposed. Fits are shown for 1,4-DEB (fit 3, dashed lines in Fig. 3) and for 1,2-DEB (fit 9, dashed lines in Fig. 5). Fits for EB and 1,3-DEB look similar and are not shown. Again, in fitting the data, the ratios $A_a/\tilde{A}_a$ and $A_{aa}/\tilde{A}_{aa}$ are kept the same and indicated as $A/\tilde{A}$ in Table I. Although the fits are successful, these fitted ratios $A/\tilde{A}$ are far too small. A ratio $A/\tilde{A} > 1$ can result because $\tilde{A}$ does not take into account proton–proton interactions between ethyl and nonethyl protons on the same molecule or intermolecular proton–proton interactions. A ratio significantly less than unity (within experimental error) is, however, impossible since the theoretical value $\tilde{A}$ is a lower limit. The fitted ratios of about 0.5 allow us to completely rule out this dynamical model. Making E_m and E_e slightly different will have a small effect.

One further model is considered for completeness. If we assume that the ethyl groups are reorienting rapidly on the nuclear magnetic resonance time scale (i.e., $\tau_e = 0$) then the *form* of the relaxation equation is identical to Eq. (17). It is obtained from Eq. (18) by setting the first and third terms to zero since $q(\tau_e) = 0$ as does $q(\tau_{em})$ since $\tau_{em} = 0$ if τ_e does [see Eq. (5)]. In this case, the fitted ratio of $A_m/\tilde{A}_m$ is greater than 3 for all four molecules as indicated in Table I for fit 4 for 1,4-DEB and fit 10 for 1,2-DEB. The actual fits are *identical* to fits 2 (Fig. 3) and 7 (Fig. 5), respectively, but the magnitude of $A_m/\tilde{A}_m$ rules out this model in practice.

V. DISCUSSION

The results of the SSPSR experiments reported here suggest that only the methyl groups in EB and the three isomers of DEB are reorienting on the nuclear magnetic resonance time scale. Whereas t-butyl groups in closely related

t-butyl benzenes do reorient in the solid state at rates comparable with their constituent out-of-plane methyl groups,[18,30,32–34] ethyl (and isopropyl) groups have a lower symmetry than t-butyl groups. During crystallization, neighboring molecules can approach the molecule nearer at the ethyl, nonmethyl proton positions than they can at the methyl positions. Ethyl group reorientation could then be strongly hindered in the solid state. Based on experiments in t-butyl systems, we can conclude that in order to appear motionless on the nuclear magnetic resonance time scale in these SSPSR experiments, the barrier for ethyl group reorientation must be larger than 50 kJ/mol, which is to be compared with the value of 5.0 $\pm$ 0.4 kJ/mol in the free molecule as determined by measuring J splittings in high resolution NMR spectroscopy[35] and 4.85 kJ/mol (no uncertainty quoted) as determined by entropy and heat capacity measurements.[36]

The SSPSR experiments in 1,3-DEB and 1,2-DEB can be interpreted in terms of two methyl group sites (a five-parameter fit) or a continuous distribution of methyl group sites (a four-parameter fit). In the continuous-distribution model, the width of the distribution of barriers $\mathscr{E}$ is very narrow. The distribution of $\mathscr{E}$ values is given by Eq. (16) and is plotted in Fig. 6 for cutoff activation energy $E = 13$ kJ/mol, distribution parameter $\epsilon = 0.85$, and $T = 100$ K. The plots for 77 and 250 K are not appreciably different from that shown in Fig. 6. The distribution Γ approaches infinity as $\mathscr{E} \to E$, but has unit area (a logarithmic singularity). The limit $\epsilon \to 1$ corresponds to a Dirac δ function at $\mathscr{E} = E$; i.e., a unique activation energy. The small difference between the two activation energies in the two-site model (i.e., two δ functions instead of the distribution shown in Fig. 6) is much larger than the "width" resulting from the continuous distribution model, but the uncertainties in the two E values in the two-site model are appreciable as indicated in Table I (fits 6 and 8). A two-site model suggests two distinct ethyl group environments per unit cell. A continuous distribution model with such a small distribution of barriers either suggests three or more *very* similar sites or a single site plus a low intensity (i.e., very few molecules) distribution of lower barriers due to molecules near dislocations, boundary edges, etc. Distinguishing between the two models or sorting out the precise interpretation of the continuous distribution model would require considerably more information than is available from SSPSR experiments.

In the absence of intermolecular interactions, the intramolecular barrier for methyl reorientation in the molecules studied here should be about 12 kJ/mol, about 4 kJ/mol for each of the three eclipsed bonds.[37] This is consistent with the observed barriers in EB, 1,3-DEB, and 1,2-DEB (Table I). 1,4-DEB is discussed below. The only comparison we can make with previously determined barriers for intraethyl methyl groups is to compare our value of 13.2 $\pm$ 0.7 kJ/mol in EB with the value of 17.15 kJ/mol (no uncertainties given) as determined from entropy and heat capacity measurements.[36]

Methyl barriers in the range of 12 kJ/mol for EB, 1,2-DEB, and 1,3-DEB imply that the ethyl groups are well away from the plane and probably in or near the orthogonal

position (as in Fig. 1). For 1,2-DEB, it also implies that the two ethyl groups are in the *anti* position. If these conclusions were not so, the methyl group barriers would be significantly higher due to steric interactions with other protons in the molecule *and* the observed values of $\widetilde{A}/A$ in the SSPSR experiments would be significantly larger than about one (see Table I). We cannot distinguish between the *anti* and the *syn* positions for 1,3-DEB and 1,4-DEB since both geometries are nearly equal in energy for the isolated molecule. It may very well be, however, that in the crystalline state, one is preferred. It would be useful and interesting to do a crystal structure for EB and all three isomers of DEB. This should be done at several temperatures.

The barriers observed in this study suggest that the intermolecular interactions in the solid play a minor role in determining the barrier for the methyl group. These conclusions are in agreement with low-resolution microwave spectroscopy studies[38,39] which have determined that the ethyl group in several ethylbenzenes sits in the "orthogonal" position. Our results are also consistent with a supersonic molecular jet spectroscopy study[40,41] which showed that there is only one conformation in 1,2-DEB, whereas there are two conformations in 1,3-DEB and 1,4-DEB (*anti* and *syn*). However, the conclusion from the supersonic molecular jet spectroscopy experiments that the *anti* form for 1,2-DEB is the one present is based solely on the independent knowledge that it is energetically more favorable. Neither the low-resolution microwave technique nor the supersonic molecular jet laser spectroscopy technique give the ground electronic state barriers for methyl group reorientation in these molecules. Finally, we note for completeness that for hexaethylbenzene, the ethyl groups alternate above and below the plane of the ring (i.e., each pair is *anti*). This is known from both from ^{13}C chemical shielding experiments[42] and x-ray diffraction.[43]

The activation energy of 9.3 ± 0.2 kJ/mol for 1,4-DEB is significantly lower than the intramolecular value of about 12 kJ/mol. One possibility is that the intermolecular contribution to the electrostatic barrier is negative (or out of phase with the intramolecular component) in the sense that it raises the minimum of the 12 kJ/mol intramolecular contribution by about 3 kJ/mol, resulting in a 9 kJ/mol barrier. This highly symmetric molecule might pack quite differently than the other isomers of DEB.

ACKNOWLEDGMENTS

[1] A. M. I. Ahmed and R. G. Eades, J. Chem. Soc. Faraday Trans. 2 68, 1337 (1972).
[2] J. Haupt and W. Müller-Warmuth, Z. Naturforsch. Teil A 24, 1066 (1969).
[3] K. Takegoshi, F. Imashiro, T. Tereo, and A. J. Saika, J. Chem. Phys. 80, 1089 (1984).
[4] P. A. Beckmann and S. Clough, J. Phys. C 10, L231 (1977).
[5] S. Clough and A. Heidemann, J. Phys. C 13, 3585 (1980).
[6] J. Kowalewski and T. Liljefors, Chem. Phys. Lett. 64, 170 (1979).
[7] U. Berg, T. Liljefors, C. Roussel, and J. Sandström, Acc. Chem. Res. 18, 80 (1985).
[8] J. Sandström, *Dynamic NMR Spectroscopy* (Academic, New York, 1982).
[9] M. Ōki, *Applications of Dynamic NMR Spectroscopy to Organic Chemistry* (VCH, Deerfield Beach, Fl., 1985).
[10] W. J. E. Parr and T. Schaefer, Acc. Chem. Res. 13, 400 (1980).
[11] A. Heidemann, M. Prager, and M. Monkenbusch, Z. Phys. B 76, 77 (1989).
[12] N. Le Calvé, D. Cavagnat, and F. Fillaux, Chem. Phys. Lett. 146, 549 (1988).
[13] D. Cavagnat, A. Magerl, C. Vettier, and S. Clough, J. Phys. C 19, 6665 (1986).
[14] W. J. Hehre, L. Radom, P. V. R. Schleyer, and J. A. Pople, *Ab Initio Molecular Orbital Theory* (Wiley, New York, 1986).
[15] R. Zallen, *The Physics of Amorphous Solids* (Wiley, New York, 1983).
[16] C. Alba, L. E. Busse, D. J. List, and C. A. Angell, J. Chem. Phys. 92, 617 (1990).
[17] D. Turnbull and M. H. Cohen, J. Chem. Phys. 34, 120 (1961).
[18] P. A. Beckmann, R. M. Hathorn, and F. B. Mallory, Mol. Phys. 69, 411 (1990).
[19] D. E. Woessner, J. Chem. Phys. 36, 1 (1962).
[20] L. K. Runnels, Phys. Rev. A 134, 28 (1964).
[21] R. L. Hilt and P. Hubbard, Phys. Rev. A 134, 392 (1964).
[22] J. D. Cutnell and W. Venable, J. Chem. Phys. 60, 3795 (1974).
[23] A. Abragam, *The Principles of Nuclear Magnetism* (Oxford University, Oxford, 1961).
[24] P. A. Beckmann, Phys. Rep. 171, 85 (1988).
[25] S. Albert, H. S. Gutowsky, and J. A. Ripmeester, J. Chem. Phys. 56, 3672 (1972).
[26] N. Bloembergen, E. M. Purcell, and R. V. Pound, Phys. Rev. 73, 679 (1948).
[27] H. Wachtel, H. Port, and H. C. Wolf, Chem. Phys. Lett. 135, 406 (1987).
[28] D. W. Davidson and R. H. Cole, J. Chem. Phys. 19, 1484 (1951).
[29] K. G. Conn, P. A. Beckmann, C. W. Mallory, and F. B. Mallory, J. Chem. Phys. 87, 20 (1987).
[30] A. M. Albano, P. A. Beckmann, M. E. Carrington, E. E. Fisch, F. A. Fusco, A. E. O'Neill, and M. E. Scott, Phys. Rev. B 30, 2334 (1984).
[31] T. Sakai, Acta Crystallogr. Sect. B 34, 3649 (1978).
[32] P. A. Beckmann, A. M. Cheung, E. E. Fisch, F. A. Fusco, R. E. Herzog, and M. Narasimhan, J. Chem. Phys. 84, 1959 (1986).
[33] P. A. Beckmann, Chem. Phys. 63, 359 (1981).
[34] P. A. Beckmann, Phys. Rev. B 39, 12248 (1989).
[35] T. Schaefer, L. Kruczynski, and W. Niemczura, Chem. Phys. Lett. 38, 498 (1976).
[36] A. Miller and D. W. Scott, J. Chem. Phys. 68, 1317 (1978).
[37] S. W. Pine, *Organic Chemistry* (McGraw–Hill, New York, 1987).
[38] N. S. True, M. S. Farag, R. K. Bohn, M. A. MacGregor, and J. Radhakrishnan, J. Phys. Chem. 87, 4622 (1983).
[39] M. S. Farag, Diss. Abstr. Int. B 35, 1594 (1974).
[40] P. J. Breen, E. R. Bernstein, and J. I. Seeman, J. Chem. Phys. 67, 3269 (1987).
[41] J. I. Seeman, H. V. Secor, P. J. Breen, V. H. Grassian, and E. R. Bernstein, J. Am. Chem. Soc. 111, 3140 (1989).
[42] S. Pausak, J. S. Tegenfeldt, and J. S. Waugh, J. Chem. Phys. 61, 1338 (1974).
[43] H. K. Pal and A. C. Guha, Z. Kristallogr. A 92, 392 (1935).